

V393
.R46

Report 1851

MIT LIBRARIES



3 9080 02753 0309



DEPARTMENT OF THE NAVY

HYDROMECHANICS



AERODYNAMICS



STRUCTURAL
MECHANICS



APPLIED
MATHEMATICS

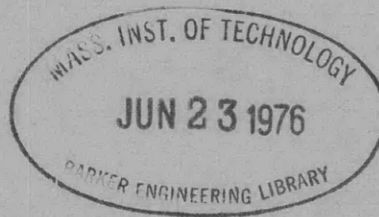


ACOUSTICS AND
VIBRATION

HYDROSTATIC PRESSURE TESTS OF
GLASS-REINFORCED PLASTIC CYLINDERS
WITH A TITANIUM JACKET

by

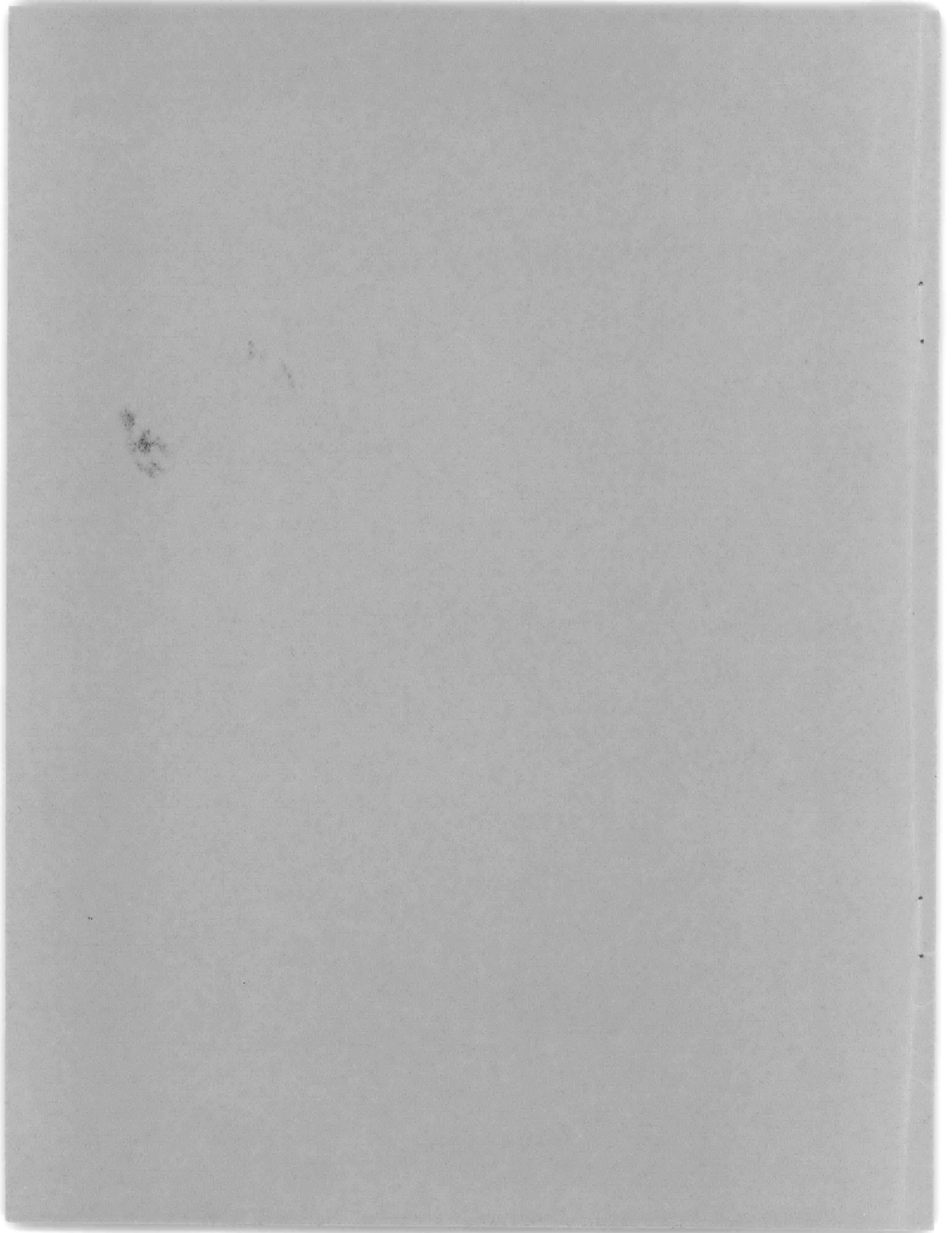
John L. Proffitt



STRUCTURAL MECHANICS LABORATORY
RESEARCH AND DEVELOPMENT REPORT

January 1965

Report 1851



HYDROSTATIC PRESSURE TESTS OF
GLASS REINFORCED PLASTIC CYLINDERS
WITH A TITANIUM JACKET

by

John L. Proffitt

January 1965

Report 1851
S-F013 01 03
S-F013 05 03

TABLE OF CONTENTS

	Page
ABSTRACT	1
ADMINISTRATIVE INFORMATION	1
INTRODUCTION	1
DESCRIPTION OF MODELS DSRV-15 AND -16	2
TEST PROCEDURE	4
TEST RESULTS	5
DISCUSSION AND INTERPRETATION OF RESULTS	5
CONCLUSIONS	8
ACKNOWLEDGMENTS	9
APPENDIX - HYDROSTATIC TESTS OF FOUR SMALL COMPOSITE FIBERGLASS CYLINDERS	10
REFERENCES	30

LIST OF FIGURES

	Page
Figure 1 - Models DSRV-15 and DSRV-16	17
Figure 2 - Gage Locations and Measured Strain Sensitivities for Models DSRV-15 and DSRV-16	18
Figure 3 - Pressure-Strain Plots at Center of Model DSRV-15	20
Figure 4 - Model DSRV-15 after Collapse	21
Figure 5 - Model DSRV-16 before, during and after Testing	22
Figure 6 - Typical Midbay Stress Cycle for Model DSRV-15	23
Figure 7 - Models DSRV-11, DSRV-12, DSRV-13, and DSRV-14	24
Figure 8 - Gage Locations and Measured Strain Sensitivities for Models DSRV-11, DSRV-12, DSRV-13, and DSRV-14	26
Figure 9 - Model DSRV-11 before and after Collapse	29
Figure 10 - Models DSRV-12, DSRV-13, and DSRV-14 after Collapse ...	29

LIST OF TABLES

	Page
Table 1 - Theoretical Collapse Pressures for Ring-Stiffened Cylinders Composed of Materials under Current Investi- gation	13
Table 2 - Comparison of Theoretical and Experimental Shell Stresses at Collapse for Models DSRV-15 and DSRV-16	14
Table 3 - Assumed Moduli, Poisson's Ratios and Elastic Buckling Pressures for Models DSRV-11, DSRV-12, DSRV-13 and DSRV-14	15
Table 4 - Comparison of Theoretical Experimental Shell Stresses at Collapse for Models DSRV-11 and DSRV-12	15
Table 5 - Comparison of Theoretical and Experimental Shell Stresses at Collapse for Models DSRV-13 and DSRV-14	16

ABSTRACT

Two cylindrical models were tested under hydrostatic pressure to determine the structural behavior of hulls composed of ring-stiffened, glass-reinforced plastic (GRP) cylinders surrounded by a thin titanium jacket and designed for a collapse depth of 30,000 ft. From these tests it was determined that composite fiberglass construction is feasible for deep-depth application from a static strength aspect. Furthermore, these tests indicate that composite fiberglass hulls offer higher static strength-weight characteristics than any metallic hulls currently under investigation. However, there is still a need for investigation of hull penetrations and end closures and the effect of cyclic and long-term loading on the collapse strength of such structures.

ADMINISTRATIVE INFORMATION

This investigation was conducted under the joint sponsorship of Bureau of Ships Codes 442 and 634 C, project nos. S-F013 01 03, Task 0214, and S-F013 05 03, Task 1025.

INTRODUCTION

In the near future, military personnel and civilian oceanographers will be seeking submersible vehicles capable of operating at greatly increased depths. To meet this demand, designers must study new materials with higher strength-to-weight ratios than those currently used for submarine pressure hulls. Studies are being conducted on high-strength metals to determine their feasibility for submarine construction. Another material which shows promise in this application is glass-reinforced, filament-wound plastic (fiberglass) which is nonweldable.

To utilize these materials efficiently, new methods of construction must be investigated. One method that is well suited to nonweldable materials is composite construction. Basically, composite construction consists of a thin jacket surrounding rings of high-strength materials. The jacket holds the rings in place and provides watertight integrity, longitudinal strength, and protection from corrosion; the rings provide the major resistance to external pressure. A more complete description of

composite design and construction is given in Reference 1.* Earlier tests conducted at the Model Basin on metallic models of composite construction gave very encouraging results.² To further investigate the feasibility of composite construction and to study the properties of fiberglass pressure hulls, two composite cylindrical models (designated Models DSRV-15 and DSRV-16) were designed at the Model Basin for an operating depth of 15,000 ft and tested to determine their elastic behavior and structural characteristics. The findings of this investigation are summarized here.

DESCRIPTION OF MODELS DSRV-15 AND -16

The two models (see Figure 1) were fabricated as part of a feasibility study of composite fiberglass submarine pressure hulls capable of operating at depths up to 15,000 ft. A collapse depth of 30,000 ft was established because of lack of adequate creep and fatigue data preceding the design of these models. It was assumed that a projected 9-ft-diameter research vehicle would utilize a 3/8-in.-thick titanium jacket surrounding the fiberglass ring-stiffened cylinder. An average fiberglass circumferential stress of 90,000 psi at collapse was assumed in the design of the models. For both models, the ratio of weight of material to weight of displaced water was 0.58.

Earlier, four smaller preliminary models had been designed and tested to aid in selecting an optimum geometry for Models 15 and 16. The results of these earlier tests are presented in the Appendix.

Based on the collapse pressures obtained with the four preliminary models, it was determined that the frame areas of Models 15 and 16 must be kept to a minimum to insure lower bending stresses in the shell without sacrificing adequate resistance to the general instability mode of failure. The elastic general instability pressure³ for a ring-stiffened cylinder is composed of two terms: the "shell-term," i.e., the assumed membrane contribution to the buckling strength of the cylinder, and the "frame term,"

*References are listed on page 30.

i.e., the bending contribution to the buckling strength. This second term was computed for a free ring having a combined cross section of the frame and effective length of shell. By providing sufficient length between restraining bulkheads, the first term can be virtually eliminated from the critical pressure calculation. This was true in the case of Models DSRV-15 and DSRV-16 since the ratio of length between bulkheads to diameter was 4.0.

Model DSRV-15 was designed with a geometry incorporating frames having the minimum area necessary for the required margin against general instability failure. The design of Model 16 provided a somewhat higher margin of general instability; the shell was sufficiently thick to lower bending stresses below those obtained in the four earlier models, however. The calculated elastic general instability pressures for Models DSRV-15 and DSRV-16 were 13,000 and 15,800 psi, respectively, assuming a modulus of 5.25×10^6 psi.

The titanium end rings for both models were originally designed to be the same depth as the fiberglass frames. However, Model DSRV-16, which was tested first, failed at the end ring-cylinder juncture. Inspection of the area of failure revealed that the fiberglass cylinder had sheared off at the juncture with the ring. This was attributed to the disparity of assumed moduli between the ring and cylinder (17×10^6 and 5.25×10^6 psi, respectively).

The incompatibility of deflections between the titanium bulkhead and the fiberglass cylinder caused high bending and shear stresses at the juncture. After the test of Model 16, the end rings of Model 15 were machined to a smaller depth as shown in Figure 1a to achieve closer compatibility of deflections, thus reducing shear stresses in the end region.

The models were fabricated by the H. I. Thompson Fiber Glass Company (HITCO) of Gardena, California, from glass-reinforced, filament-wound plastic. A preimpregnated roving* consisting of S-HTS glass and

*A roving consists of 20 "ends" each containing 100 to 120 individual glass fibers preimpregnated with resin. The roving is unwound from a spool in a manner very similar to that for yarn.

an E-787 resin system was used. With a prescribed tension of 5 to 9 lb, the glass fibers were wound onto a mandrel coated with a heat-resistant mold release. Circumferential fibers were wound directly on the model mandrel, and longitudinal filaments were wound on another, larger mandrel in a layer one or two plies thick, cut lengthwise to the mandrel and spread flat into sheets that were applied to the model. For each model, two 28-in.-long cylinders were manufactured by winding five plies of circumferential fibers, hand placing one ply of longitudinal filaments, and then repeating the process until 38 plies had been placed. Next the surface was covered with shrink tape and cured 2 hr at 225 F and 3 hr at 325 F. The overwrap was removed and 41 plies were placed, once again in a 5-to-1 filament orientation. Then the cylinder was cured as before and two more stages of winding were completed, this time with a 2-to-2 filament orientation. After final curing for 2 hr at 225 F and then 10 hr at 325 F, the cylinder was machined to the proper outside diameter and removed from the mandrel. Then two 11-in. ring-stiffened cylinders were finished from each 28-in. cylinder. Three frame units were also machined from the two 28-in. cylinders. Next, one titanium end ring was welded to the titanium jacket. Finally, the completed fiberglass and titanium components were slipped into the jacket subassembly and the second titanium end ring was welded to the jacket. An identical procedure was followed for the second model.

TEST PROCEDURE

After instrumentation with foil resistance gages (see Figure 2), Models 15 and 16 were tested in the gun barrel pressure tank at the Model Basin. On the first run, these models were subjected to a pressure of 3300 psi (one-half operating pressure) in 300-psi increments; the models were then removed from the tank and the jacket examined for buckling. In the next pressure run, the models were taken up to operating pressure (6600 psi) in 600-psi increments; then the models were again removed from the tank and inspected for buckling in the jacket. In the final pressure run the models were tested to collapse; up to 6000 psi, pressure was applied in 3000-psi increments, and above 6000 psi, the loading rate was held as close as practicable to 100 psi/min until collapse occurred. Strain data were automatically recorded during the three pressure runs.

TEST RESULTS

Models DSRV-15 and DSRV-16 collapsed at pressures of 14,300 and 11,590 psi, respectively. Strain sensitivities for both models are included in Figure 2; they are the average value of the first and second pressure runs. Failure occurred at the first interior joint on Model 15 and at the end joint on Model 16. Examination of the jackets after pressures of 3300 and 6600 psi had been applied failed to show any premature buckling of the jacket. For Model 15, all pressure-strain plots were linear with the exception of the circumferential strains at the model's center; Figure 3 shows pressure-strain plots obtained during the third pressure run for the frame gages at the center of the model. Pressure-strain plots for Model 16 were linear up to failure. Figure 4 shows Model 15 after collapse; Figure 5 shows Model 16 before, during, and after testing.

DISCUSSION AND INTERPRETATION OF RESULTS

Failure of Model DSRV-15 occurred at the first cylinder juncture at a pressure of 14,300 psi or 107 percent of design pressure. Model DSRV-16 collapsed at the end ring-cylinder juncture at a pressure of 11,590 psi or 87 percent of design collapse pressure.

These results clearly indicate that composite fiberglass construction of pressure hulls is indeed attractive from a static strength viewpoint, and it is of interest to compare the collapse pressures with those obtained for metallic cylinders. Three materials are currently under investigation for use in metallic pressure hulls:

Material	Yield strength in psi
Steel	150,000 - 200,000
Titanium	110,000 - 150,000
Aluminum	60,000

Collapse pressures for ring-stiffened metallic cylinders can be approximated by applying the simple hoop stress equation if it is assumed that required instability pressures are satisfied by judicious distribution of the material. This hoop stress concept is substantiated by actual model

tests.^{1,2,4} Using the upper bound of the yield strength of the above mentioned materials and selecting a weight-to-displacement ratio identical to Model DSRV-15, Table 1 compares the collapse pressures for metallic cylinders with the experimental collapse pressure of this fiberglass cylinder. It is evident from this table that the static strength performance of this composite fiberglass hull is superior to any metallic hull currently under consideration.

Evidence of bifurcation of recorded circumferential strains at the center of Model DSRV-15 (Figure 3) is very slight; it would be difficult to predict a general instability pressure accurately from such data. Because the model did exceed the design collapse pressure, it is safe to assume that the general instability pressure was sufficient but not excessive since it should be remembered that the calculated critical pressure was only 13,000 psi. The margin of error can probably be attributed to a conservative value of the elastic modulus (5.25×10^6) chosen for the calculation.

The combined axial plus bending stress on the inside surface of the cylinder at the ring-cylinder juncture can be calculated by using measured deflections and assuming no rotation of the joint.⁵ This value was calculated to be 146,500 psi at collapse for Model 16 compared to 137,600 psi at collapse for Model 15.

A comparison of experimental and theoretical stresses at collapse using graphical means of solution,^{6,7} shows fairly close correlation for both models; see Table 2. For this analysis, the titanium jacket was assumed to act monolithically with the fiberglass shell. The effective shell thickness was considered to be the actual shell thickness plus the jacket thickness multiplied by the ratio of the jacket modulus (17.0×10^6 psi) to the shell modulus (5.25×10^6). The frames were assumed to have a modulus of 7.0×10^6 psi (because of their 5-to-1 circumferential to longitudinal filament orientation), necessitating an adjustment in their areas for the purpose of the stress analysis. The actual area was multiplied by the ratio of the frame modulus to the shell modulus and by the ratio of the shell centroidal radius to the frame centroidal radius.

The fact that no permanent set was recorded on the jacket gages after completion of the first two pressure runs (to 6600 psi) indicates

that the jacket was not in a state of residual tension. Jacket tension at zero pressure is possible if the jacket yields when pressure is applied to and released from a composite cylinder composed of a higher modulus jacket material and a lower modulus shell and frame material, as explained in Reference 1. The reason there was no permanent jacket set appears to be that the yield strength of the jacket was not reached upon application of 6600 psi of pressure. The calculated circumferential midbay stress at that pressure was 116,000 psi, 4000 psi below the nominal yield strength of the 6AL4V titanium alloy used for the jacket. Figure 6 shows the midbay stress cycle for Model DSRV-15. It is very possible also that the actual yield strength of the alloy was considerably higher than the nominal value; unfortunately, no stress-strain curves were available for this material. Because a residual tensile stress of low magnitude is desirable to secure a tight fit between jacket and shell, it would be advantageous to employ a jacket material with a yield strength of 100,000 to 110,000 psi. However, large residual tensile stresses are to be avoided because of the possibility of fatigue failure. On larger scale models and prototype vehicles, residual tensile stresses of weldments must also be considered.

Several advantages of composite fiberglass construction are apparent even from this rather preliminary investigation. The most evident advantage is the protection from corrosion offered by the metal jacket. Sea water is prevented from contaminating the fiberglass cylinders, which may be susceptible to deterioration. Composite construction is advantageous in the fabrication of full-scale vehicles. Since the jacket provides structural integrity by locking the cylindrical elements in place, these elements can be manufactured to any desired length without altering their structural characteristics, thus alleviating many fabrication and handling problems. In addition, it is possible that a damaged hull section can be replaced by opening the jacket and inserting another cylinder.

The efficiency of composite fiberglass pressure hulls can be improved in several ways. Improved resin systems should give rise to higher composite stress levels and interlaminar shear strengths. In current practice, laminate compressive stresses are far below those of the glass fibers. The use of hollow glass filaments in laminates might

lead to more efficient design of pressure hulls by eliminating the need for a heavy stiffener system. The required buckling pressures might be met by using hollow filaments in an unstiffened or very lightly stiffened cylinder or a more stable shape such as a prolate spheroid (football). These approaches minimize the highly undesirable shear stresses associated with ring-stiffened geometries at the point where loads are transferred from the shell to the frame. A fiberglass "sandwich" cylinder separated by a continuous stiffener system composed of low-density core material is another type of construction which may provide better performance through the reduction of shear stresses.

Of course, it must be realized that further feasibility studies are needed to definitely establish the utility of a fiberglass pressure hull. A practical structure has to be penetrated to provide access for machinery, equipment, and personnel. At present, little is known about the behavior of a penetration in an orthotropic, nonyielding pressure cylinder. The most advantageous method of closing the end of such a cylinder must be determined. Long-term cyclic loading and the loading rate may be two factors governing the strength of a fiberglass hull. Because of the unique manufacturing technique employed for the fabrication of a fiberglass cylinder, it is not now known whether the structural characteristics of the material are adversely affected by the scale factor, i.e., whether larger, thicker sections will possess a lower allowable stress level. To initiate study of these problems, several models have been designed and fabricated which incorporate hull penetrations and end closures. Subsequent larger-scale and full-assembly models are planned for static and fatigue testing. These areas of investigation must be pursued before glass-reinforced plastic can be seriously considered as the major structural element of a deep-diving submarine pressure hull.

CONCLUSIONS

1. A pressure hull model composed of a fiberglass ring-stiffened cylinder and an HY-120 titanium jacket weighs approximately 58 percent of its displacement when designed for a collapse depth of 30,000 ft. Such a model has a better strength-weight performance than metallic hulls using materials currently under investigation.

2. Composite construction shows promise of enabling the designer to use glass-reinforced plastic as the major component for ultra-deep-depth oceanographic vehicles. A metal jacket protects the glass-reinforced plastic pressure hull from the deep-sea environment.

ACKNOWLEDGMENTS

The author wishes to express his appreciation to Mr. M. A. Krenzke for his guidance throughout the course of this investigation and to Mr. J. A. Nott for his help in calculating the theoretical sandwich model stresses. Thanks are also due to Mr. W. R. Stewart who instrumented the models and assisted in the tests and to Messrs. George D. Lee and Norbert C. Myers of the H. I. Thompson Fiber Glass Company who ably handled all problems associated with the fabrication of these models.

APPENDIX

HYDROSTATIC TESTS OF FOUR SMALL COMPOSITE FIBERGLASS CYLINDERS

Prior to the tests summarized in this report, four preliminary models (designated DSRV-11 through DSRV-14) were designed and tested to aid in selection of an optimum geometry for the two fiberglass models DSRV-15 and 16. These earlier models were made with individual frame and ring segments rather than fabricated as monolithic ring-stiffened cylinders; see Figure 7. The material used was a preimpregnated roving of E-HTS glass and E-787 resin. A thin coat of epoxy was sprayed on the models to provide watertightness.

All four models were designed with an average circumferential stress of 90,000 psi at a collapse pressure of 12,500 psi since the omission of the titanium jacket was assumed to decrease the collapse pressure by 833 psi. The shell on Models 11 and 12 had a glass filament orientation of 1 circumferential fiber to 1 longitudinal fiber, whereas the shell on Models 13 and 14 had a 3-to-2 filament orientation. Because the modulus of E type glass is lower than that of S type glass, an effective buckling modulus of 5.0×10^6 rather than 5.25×10^6 psi was assumed in the calculation of general instability pressures. These pressures were based on models of semi-infinite length. Therefore actual instability pressures for the four models would be somewhat greater. Table 3 compares general instability pressures, and the assumed moduli and Poisson's ratios used to calculate stresses for all four models. Models DSRV-11 and DSRV-12 were ring-stiffened cylinders, and each had a ratio of weight-of-material to weight-of-displacement of 0.51. The two sandwich-type construction models (DSRV-13 and DSRV-14) weighed 55.0 and 55.8 percent of their displacement, respectively.

Models 11 and 12 were tested identically. After instrumentation with foil resistance gages, the models were placed in the TMB 13-in. tank. Figure 8 shows gage locations and strain sensitivities for Models 11 through 14. Pressure was applied in 10 equal increments until a pressure of 6250 psi was reached. The pressure was released and the procedure repeated. Strain-gage data were taken with automatic recorders to study the elastic behavior of the models. Because the gages placed on the epoxy

jacket of Model 11 showed such poor correlation with their corresponding inside gages, it was decided to omit instrumentation of the outside of Models 12, 13, and 14. After initial pressure tests to 6250 psi to obtain strain measurements, Models 11 and 12 were moved to the TMB high-pressure tank (projectile) where they were tested to collapse by applying pressure in increments of 100 psi/min after initially applying 6000 psi.

Models 13 and 14 were tested in the 13-in. tank to determine their elastic behavior. However, Model 13 collapsed on its first pressure run. When Model 14 was tested, the first run was limited to 2500 psi to prevent collapse. On the second pressure run, the increments were 500 psi up to 4000 psi. From 4000 psi to collapse pressure, 100-psi increments were utilized.

Strain data taken from elastic tests of Models 11 through 14 showed a high degree of linearity for all but a very few gages. For this reason, it did not seem necessary to show pressure-strain plots for these models. Gage locations and measured strain sensitivities of these models are given in Figure 8. Model DSRV-11 collapsed at a pressure of 8600 psi; Figure 9 shows photographs of this model before and after collapse. Models 12, 13, and 14 collapsed at 7200, 4800, and 4700 psi, respectively. In each case, failure was characterized by delamination of the shell segments and shearing of the bulkhead and frame rings. Figure 10 shows photographs of Models 12, 13, and 14 after collapse.

A stress analysis using graphical means of solution⁶ was made for both ring-stiffened models, DSRV-11 and DSRV-12. The effective frame area was assumed to be the actual area multiplied by the ratio of the assumed frame circumferential modulus (7.0×10^6) to the assumed shell modulus (5.0×10^6) and then multiplied by the ratio of the centroidal radius of the shell to the frame centroidal radius. A comparison of theoretical with experimental stresses (Table 4) shows fairly poor correlation for both models, particularly in the longitudinal direction of the frame. This discrepancy can be attributed to the small scale of the models (0.0767) and the longer gage length (1/8 in.) used, giving an average strain reading over a length somewhat away from the frame.

Table 5 compares theoretical⁸ and experimental stresses at collapse on the inside surfaces of Models DSRV-13 and DSRV-14. Although the

correspondence of calculated and measured stresses leaves much to be desired for these two tests, it should be noted that both theoretical and experimental values are far below the ultimate compressive stress which glass-reinforced plastics are capable of developing. Indeed, they are well below the rather conservative 90,000 psi used for the design collapse stress.

Obviously, there is a need to establish a criterion of failure other than that of compressive shell yielding. After collapse, all four preliminary models exhibited severe delamination of the shells. This might indicate that failure was due to the high bending stresses associated with the large frame areas and relatively thin shells found in the geometries of the four models. These particular geometries were chosen because they possessed high elastic general instability pressures.³ At the cost of lowering the instability pressures somewhat, subsequent designs (Models DSRV-15 and DSRV-16, described in the body of the text) incorporated thicker shells to reduce bending and shear stresses. Also, frame areas were decreased to keep the weight-to-displacement ratios close to those of Models 11 through 14 and to reduce the effect of "hard spots" on collapse pressures.

It has been speculated that another collapse criterion in glass-reinforced plastics is that of interlaminar shear. Calculation of the shear stresses⁸ at the interface of the web and outer shell for Models DSRV-13 and DSRV-14 gave values of 6920 and 7710 psi, respectively. These values are within the range of 7000 to 9000 psi, which is about the interlaminar shear strength of currently used glass-reinforced plastics.

TABLE 1
 Theoretical Collapse Pressures for Ring-Stiffened
 Cylinders Composed of Materials under
 Current Investigation

Material	Yield Strength psi	W/D*	Collapse Pressure psi
Titanium	150,000	0.58	10,430
Steel	200,000	0.58	7,710
Aluminum	60,000	0.58	6,830
Composite GRP**	96,500**	0.58	14,300
<p>* Ratio of weight of hull to weight of water displaced by hull for a typical section.</p> <p>** Based on test results of Model DSRV-15.</p>			

TABLE 2

Comparison of Theoretical and Experimental Shell Stresses
at Collapse for Models DSRV-15 and DSRV-16

Type of Stress *	Stress at Failure		% Error $\left(1 - \frac{\sigma_{\text{exp}}}{\sigma_{\text{the}}}\right) 100$
	Theoretical ²	Experimental	
Model DSRV-15, $P_c = 14,300$			
$\sigma_{\phi \text{ om}}$	81,160	71,380	+12.1
$\sigma_{\phi \text{ im}}$	90,680	82,713	+ 9.1
$\sigma_{x \text{ om}}$	53,570	57,240	-10.7
$\sigma_{x \text{ im}}$	46,360	52,058	-11.2
$\sigma_{\phi \text{ if}}$	92,990	88,540	+ 4.8
$\sigma_{x \text{ if}}$	57,340	62,150	- 8.4
Model DSRV-16, $P_c = 11,590$			
$\sigma_{\phi \text{ om}}$	65,910	64,380	+ 2.3
$\sigma_{\phi \text{ im}}$	71,390	70,750	+ 1.6
$\sigma_{x \text{ om}}$	48,930	47,560	+ 2.8
$\sigma_{x \text{ im}}$	38,950	38,380	+ 1.5
$\sigma_{\phi \text{ if}}$	74,710	71,410	+ 4.4
$\sigma_{x \text{ if}}$	52,420	56,730	- 8.2
$E_{\phi} = E_x = 5.25 \times 10^6$ psi $\nu_{\phi} = \nu_x = 0.24$ * $\sigma_{\phi \text{ om}}$ - Circumferential, outside midbay $\sigma_{\phi \text{ im}}$ - Circumferential, inside midbay $\sigma_{x \text{ om}}$ - Longitudinal, outside midbay $\sigma_{x \text{ im}}$ - Longitudinal, inside midbay $\sigma_{\phi \text{ if}}$ - Circumferential, inside, at frame $\sigma_{x \text{ if}}$ - Longitudinal, inside, at frame			

TABLE 3

Assumed Moduli, Poisson's Ratios and Elastic Buckling Pressures for Models DSRV-11, DSRV-12, DSRV-13 and DSRV-14

Model	$E_{\phi}(x 10^{-6})$	$E_x(x 10^{-6})$	ν_{ϕ}	ν_x	$P_{cr} = \frac{3EI}{LR_0 \bar{R}^2}$
DSRV-11	5.0	5.0	0.24	0.24	15,490
DSRV-12	5.0	5.0	0.24	0.24	15,050
DSRV-13	5.5	4.5	0.26	0.22	18,380
DSRV-14	5.5	4.5	0.26	0.22	18,430

TABLE 4

Comparison of Theoretical and Experimental Shell Stresses at Collapse for Models DSRV-11 and DSRV-12

Type of Stress*	Stress at Failure		% Error $\left(1 - \frac{\sigma_{exp}}{\sigma_{the}}\right) 100$
	Theoretical	Experimental	
Model DSRV-11, $P_c = 8600$			
$\sigma_{\phi im}$	56,880	65,200	-14.6
$\sigma_{x im}$	44,470	37,320	+16.1
$\sigma_{\phi if}$	62,590	64,310	- 2.7
$\sigma_{x if}$	72,750	52,510	+27.9
Model DSRV-12, $P_c = 7200$			
$\sigma_{\phi im}$	47,440	52,850	-11.4
$\sigma_{x im}$	33,090	21,670	+34.5
$\sigma_{\phi if}$	54,310	52,160	+ 4.0
$\sigma_{x if}$	69,600	41,360	+40.6
<p>*$\sigma_{\phi im}$ - Circumferential, inside midbay</p> <p>$\sigma_{x im}$ - Longitudinal, inside midbay</p> <p>$\sigma_{\phi if}$ - Circumferential, inside at frame</p> <p>$\sigma_{x if}$ - Longitudinal, inside at frame</p>			

TABLE 5

Comparison of Theoretical and Experimental Stresses
at Collapse for Models DSRV-13 and DSRV-14

Type of Stress*	Stress at Failure		% Error $\left(1 - \frac{\sigma_{\text{exp}}}{\sigma_{\text{the}}}\right) 100$
	Theoretical	Experimental	
Model DSRV-13, $P_c = 4800$ psi			
σ_{ϕ} mii	36,000	30,400	+ 15.6
σ_x mii	31,770	30,640	+ 3.6
σ_{ϕ} fii	33,370	37,120	- 11.2
σ_x fii	11,140	15,280	- 37.2
Model DSRV-14, $P_c = 4700$ psi			
σ_{ϕ} mii	34,580	30,360	+ 12.2
σ_x mii	36,360	47,150	- 29.6
σ_{ϕ} fii	30,850	29,910	+ 3.1
σ_x fii	2,080	11,070	-432.2
σ_{ϕ} mii	Circumferential, midbay, inner shell, inside surface		
σ_x mii	Longitudinal, midbay, inner shell, inside surface		
σ_{ϕ} fii	Circumferential, at web, inner shell, inside surface		
σ_x fii	Longitudinal, at web, inner shell, inside surface		

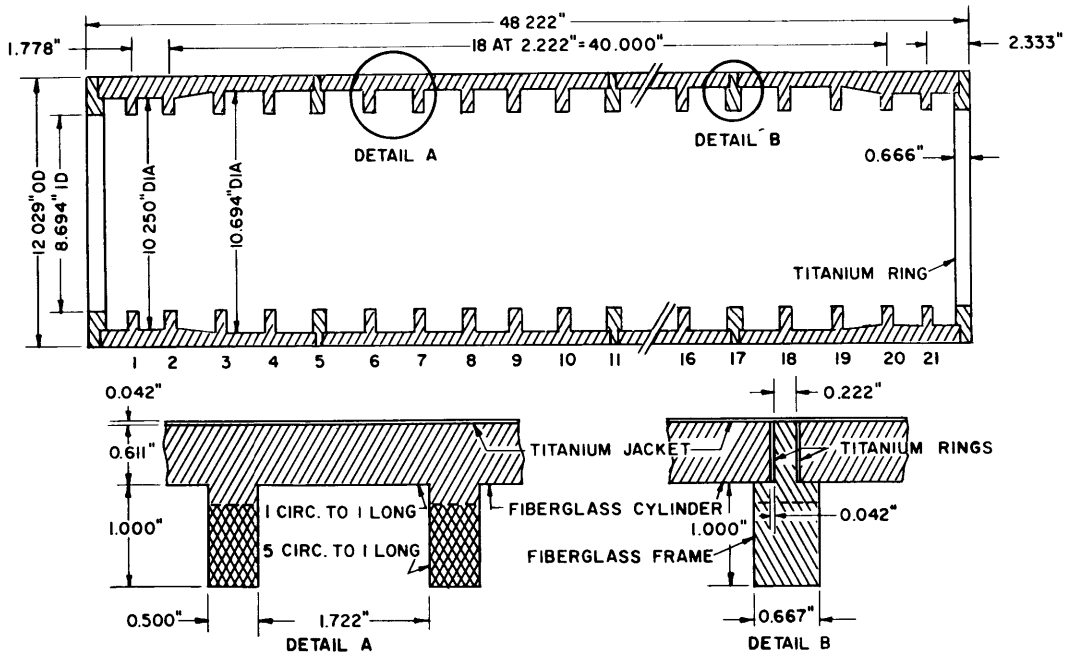
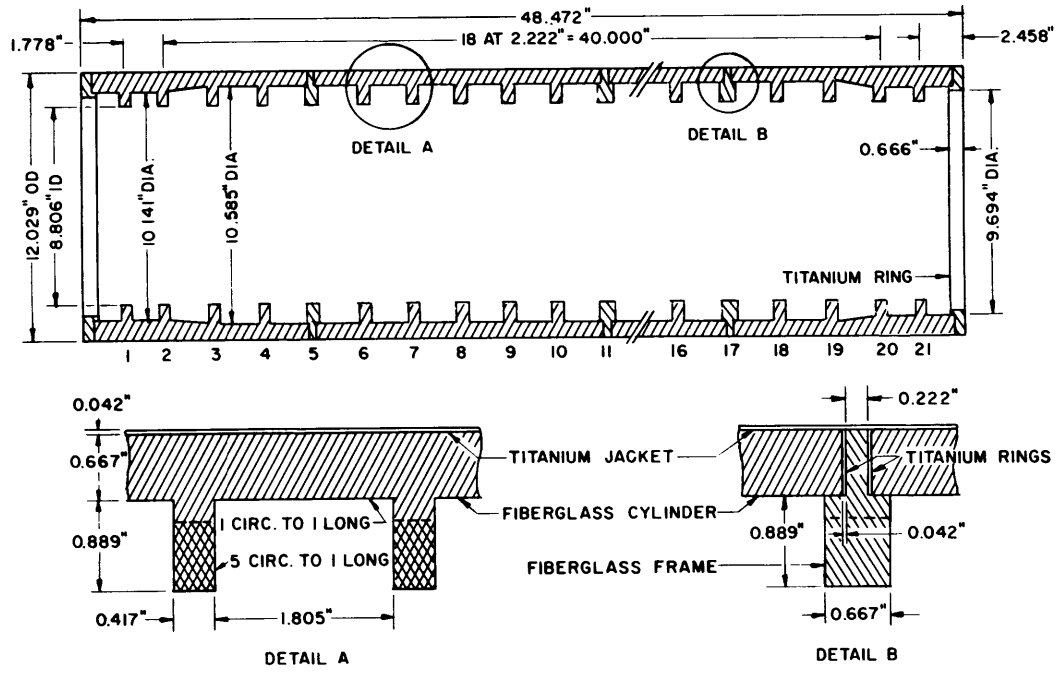


Figure 1 - Models DSRV-15 and DSRV-16

Figure 2 - Gage Locations and Measured Strain Sensitivities for Models DSRV-15 and DSRV-16

Odd numbered gages are longitudinal. Even numbered gages are circumferential

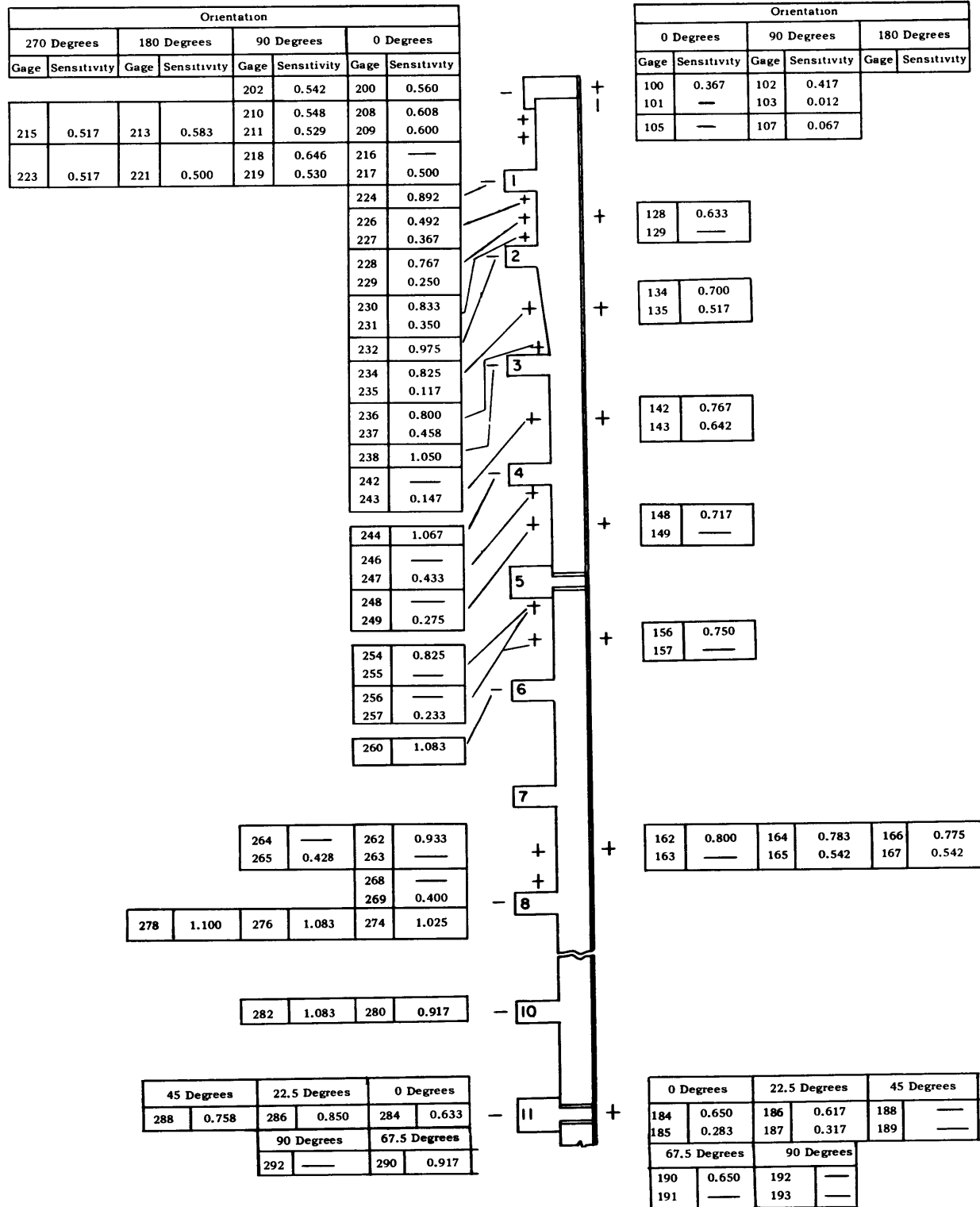


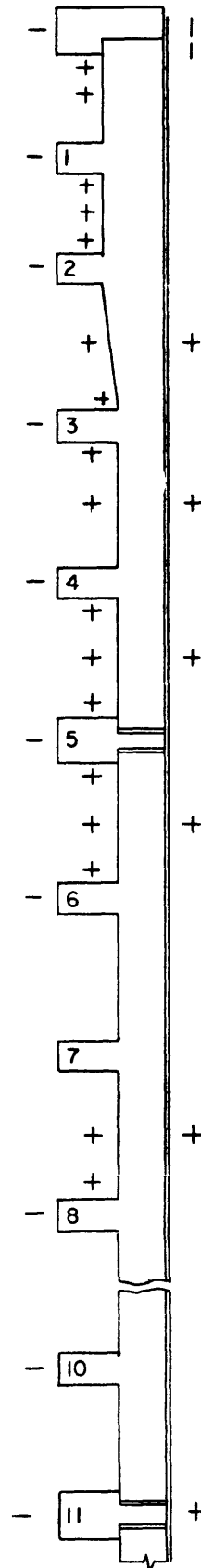
Figure 2a - Model DSRV-15

Orientation							
270 Degrees		180 Degrees		90 Degrees		0 Degrees	
Gage	Sensitivity	Gage	Sensitivity	Gage	Sensitivity	Gage	Sensitivity
				202	0.400	200	0.428
				210	0.500	208	0.442
215	0.775	213	0.592	211	0.692	209	0.758
				218	0.525	216	0.600
223	0.492	221	0.450	219	0.108	217	0.475
				224	0.817		
				226	0.700		
				227	0.408		
				228	0.800		
				229	0.308		
				230	0.833		
				231	0.367		
				232	1.017		
				234	0.900		
				235	0.275		
				236	0.850		
				237	0.875		
				238	1.058		
				240	0.892		
				241	0.733		
				242	0.983		
				243	0.392		
				244	1.100		
				246	0.917		
				247	0.542		
				248	0.925		
				249	0.375		
				250	0.833		
				251	0.567		
				252	0.917		
				254	0.833		
				255	0.458		
				256	0.917		
				257	0.367		
				258	0.900		
				259	1.600		
				260	1.083		

266	0.925	264	0.933	262	0.958
267	0.400	265	0.467	263	0.367
		270	0.900	268	0.867
		271	0.592	269	0.567
		276	1.067	274	0.900

282	1.050	280	1.033
-----	-------	-----	-------

90	67.5	45	22.5	0					
292	-	290	0.917	288	0.917	286	0.892	284	0.917



Orientation					
0 Degrees		90 Degrees		180 Degrees	
Gage	Sensitivity	Gage	Sensitivity	Gage	Sensitivity
101	-	103	0.350		
109	-	111	0.358		

134	-
135	0.525

142	-
143	0.642

148	0.758
149	-

156	0.750
157	0.592

162	0.775	164	-	166	0.775
163	0.575	165	-	167	0.550

0	22.5	45	67.5	90					
184	0.667	186	0.642	188	0.658	190	0.675	192	-
185	0.158	187	-	189	0.183	191	0.208	193	0.233

Figure 2b - Model DSRV-16

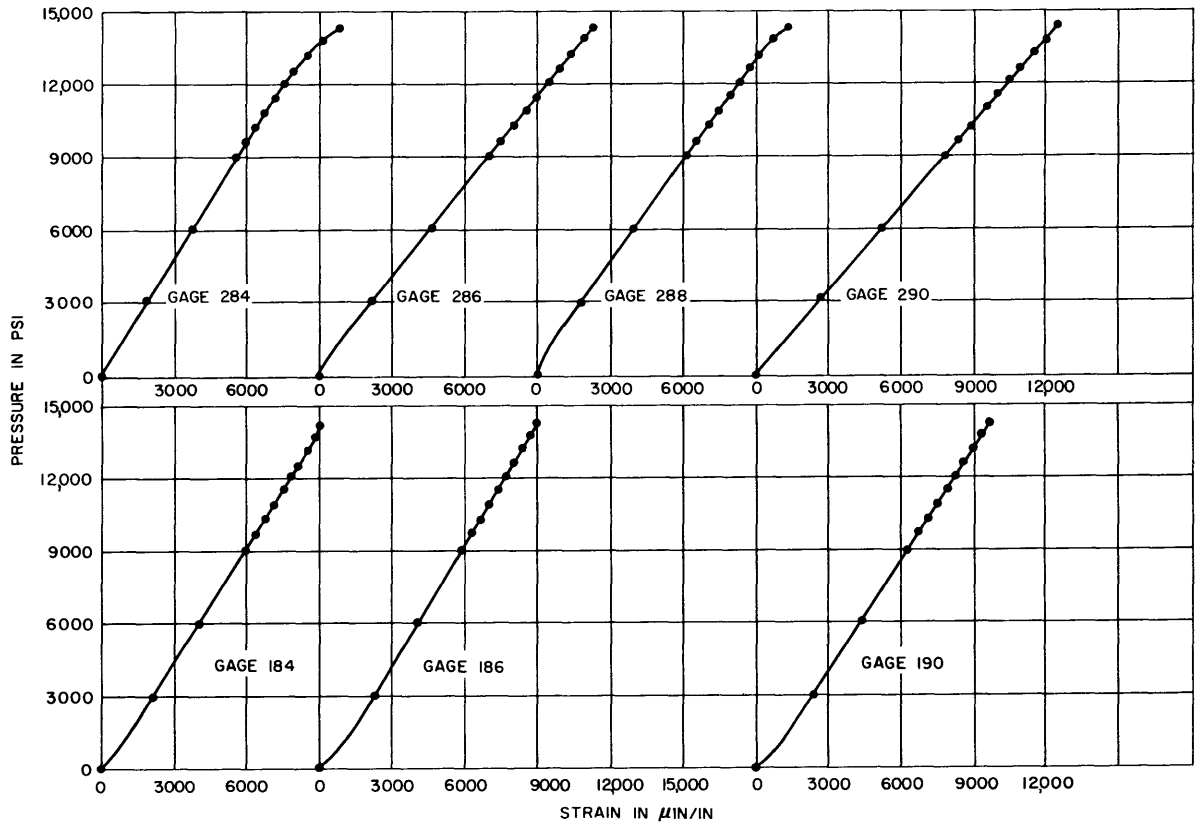


Figure 3 - Pressure-Strain Plots at Center of Model DSRV-15



Figure 4 - Model DSRV-15 after Collapse

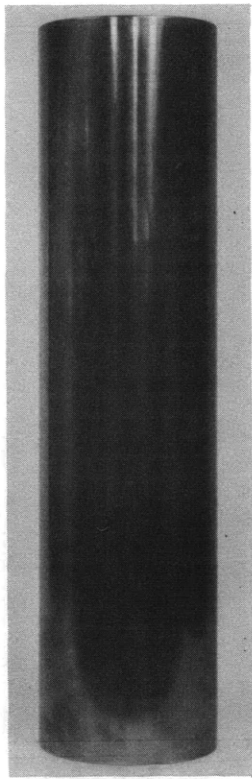


Figure 5a -
Before test

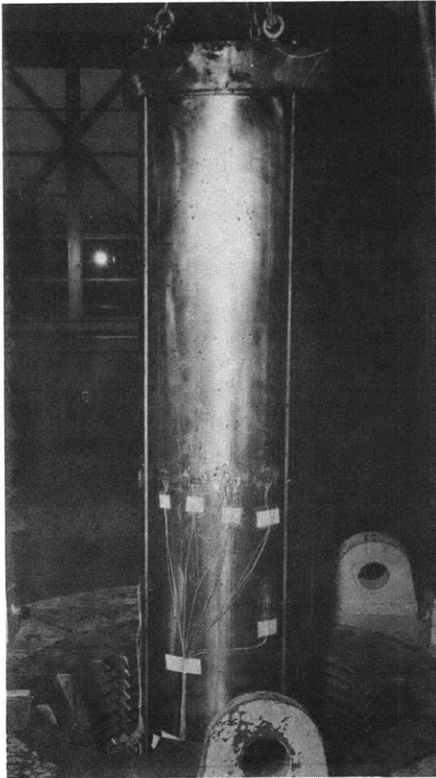


Figure 5b - After 6600-psi
Pressure



Figure 5c - After Collapse

Figure 5 - Model DSRV-16 before, during, and after Testing

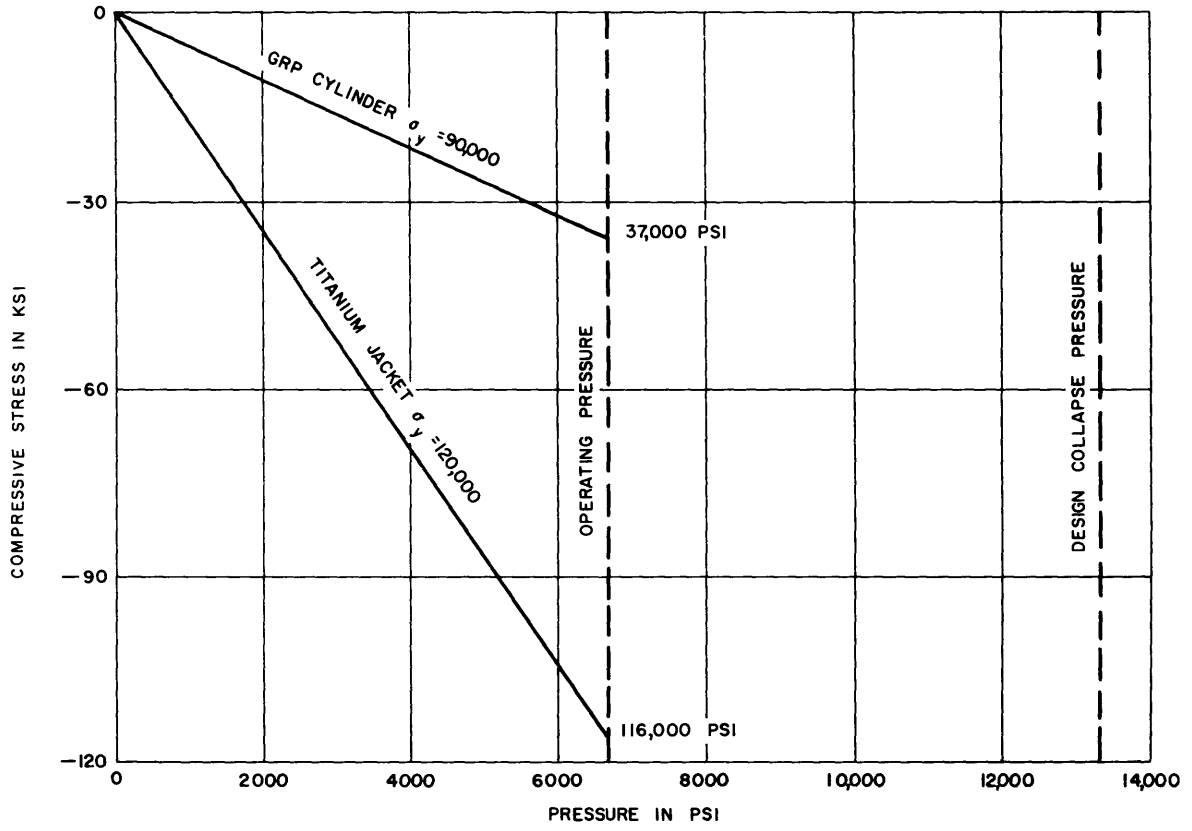


Figure 6 - Typical Midbay Stress Cycle for Model DSRV-15
 GRP Cylinder Stress Shown is the Membrane Stress.

Figure 7 - Models DSRV-11, DSRV-12, DSRV-13, and DSRV-14

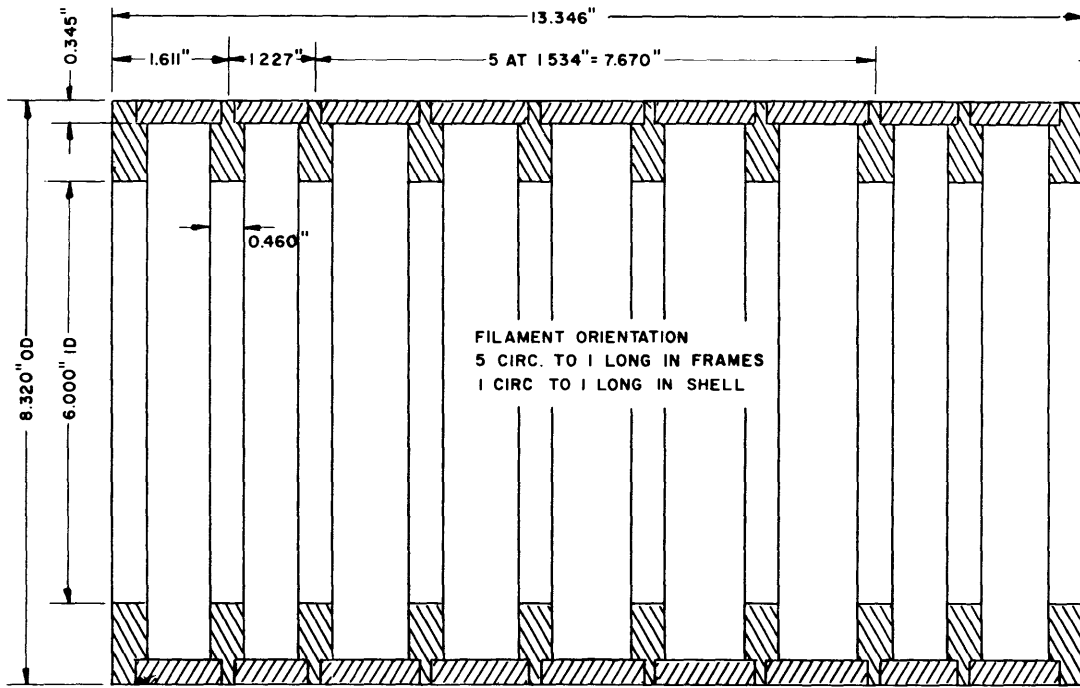


Figure 7a - Model DSRV-11

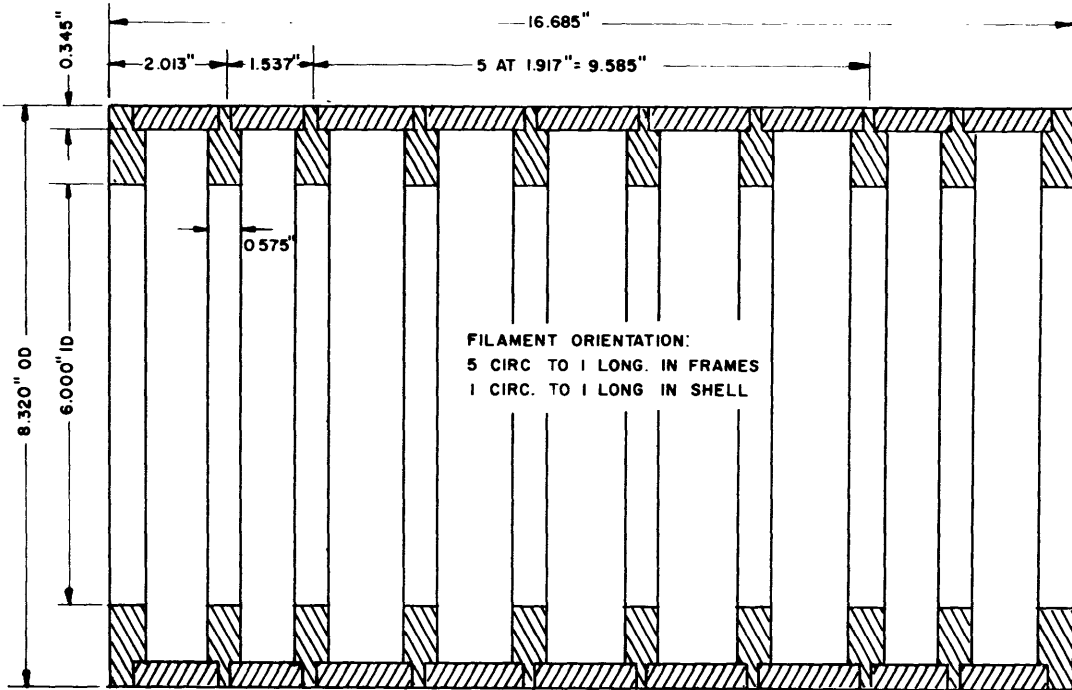


Figure 7b - Model DSRV-12

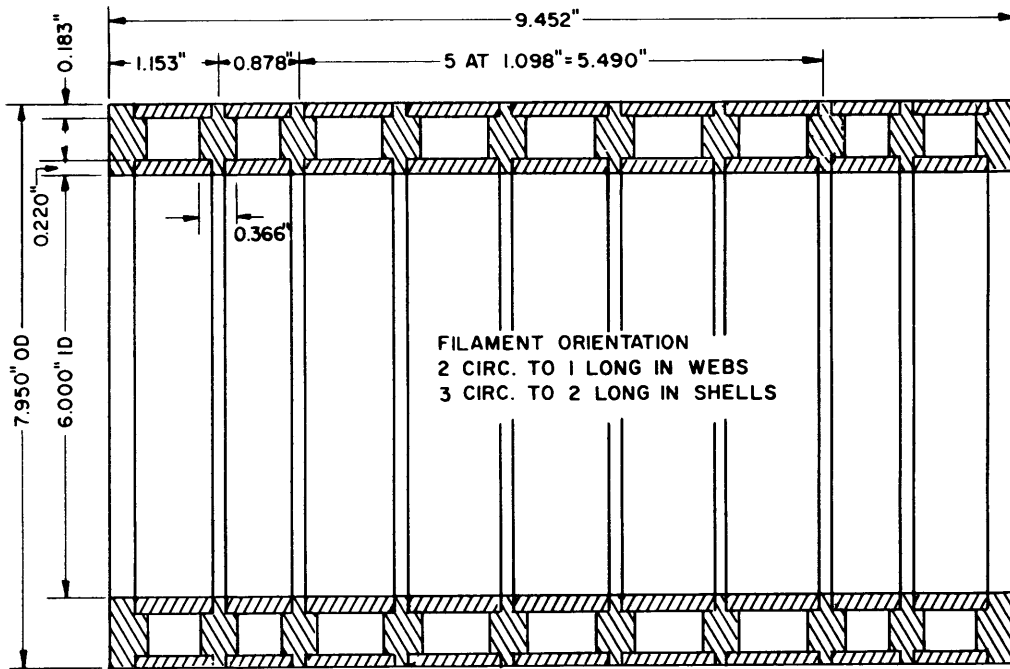


Figure 7c - Model DSRV-13

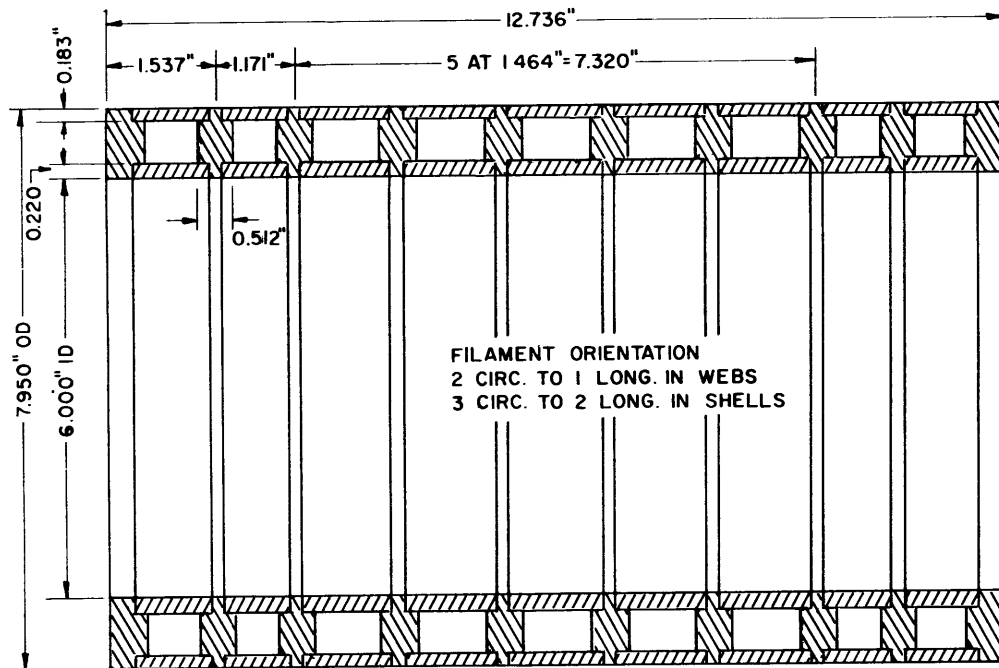
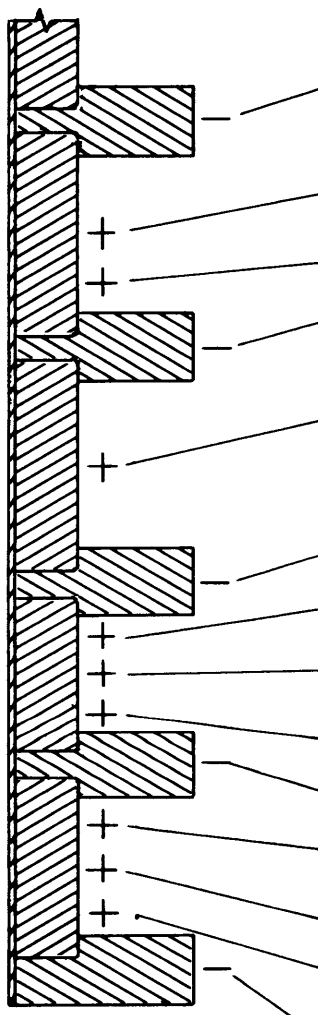


Figure 7d - Model DSRV-14

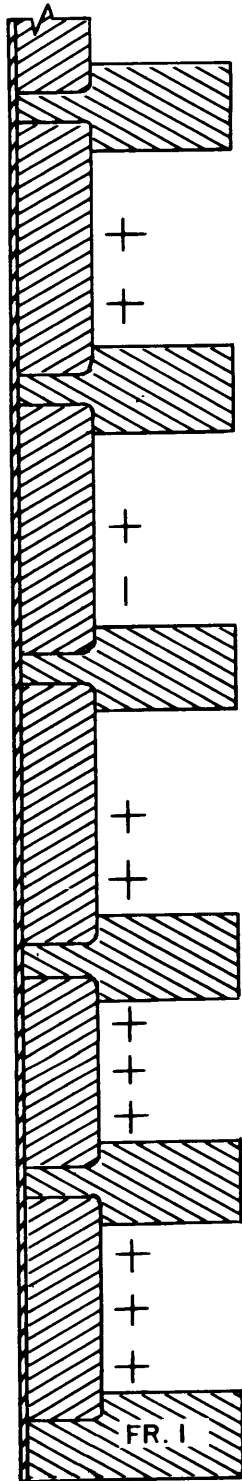
Figure 8 - Gage Locations and Measured Strain Sensitivities for Models DSRV-11, DSRV-12, DSRV-13, and DSRV-14

Even numbered gages are circumferential and odd numbered gages are longitudinal.



		Orientation							
		0 Degrees		90 Degrees		180 Degrees		270 Degrees	
Gage	Sensitivity	Gage	Sensitivity	Gage	Sensitivity	Gage	Sensitivity	Gage	Sensitivity
216	1.30	218	1.30	220	1.31	222	1.32		
200	Out	202	1.30	204	1.33	206	1.31		
201	0.12	203	0.31	205	0.56	207	0.44		
208	1.20								
209	0.58	211	0.68	213	0.72	215	0.97		
226	1.38								
228	1.30			230	1.32				
229	0.26			231	0.47				
234	1.25								
236	Out								
237	0.83								
238	0.80			240	1.12				
239	0.67			241	0.68				
242	1.10								
243	0.68			245	0.86				
246	1.22								
248	1.08								
249	0.56								
250	1.15								
251	0.27								
252	Out			256	0.94				
253	0.52	255	0.84	257	0.86	259	0.90		
260	1.00								

Figure 8a - Model DSRV-11



Orientation							
0 Degrees		90 Degrees		180 Degrees		270 Degrees	
Gage	Sensitivity	Gage	Sensitivity	Gage	Sensitivity	Gage	Sensitivity
200	1.31			202	1.32		
201	0.17			203	0.03		
204	1.16						
205	0.62			207	Out		
208	1.16	210	1.16	212	1.16	214	1.14
216	1.14	218	1.31	220	Out	222	1.31
217	0.16	219	0.25	221	Out	223	0.17
		225	0.69			227	0.55
228	1.16						
230	1.00			232	1.32		
231	0.07			233	0.08		
234	1.16						
235	0.62						
236	Out						
238	1.00						
239	0.64						
240	1.07			242	1.10		
241	0.35			243	0.28		
244	1.86						
245	0.17			247	0.33		
248	0.96						
250	0.93						
251	0.41						
252	1.16						
253	0.19						
254	0.90			258	0.62		
255	0.97	257	0.69	259	0.41	261	0.83
262	0.90						

Figure 8b - Model DSRV-12

28

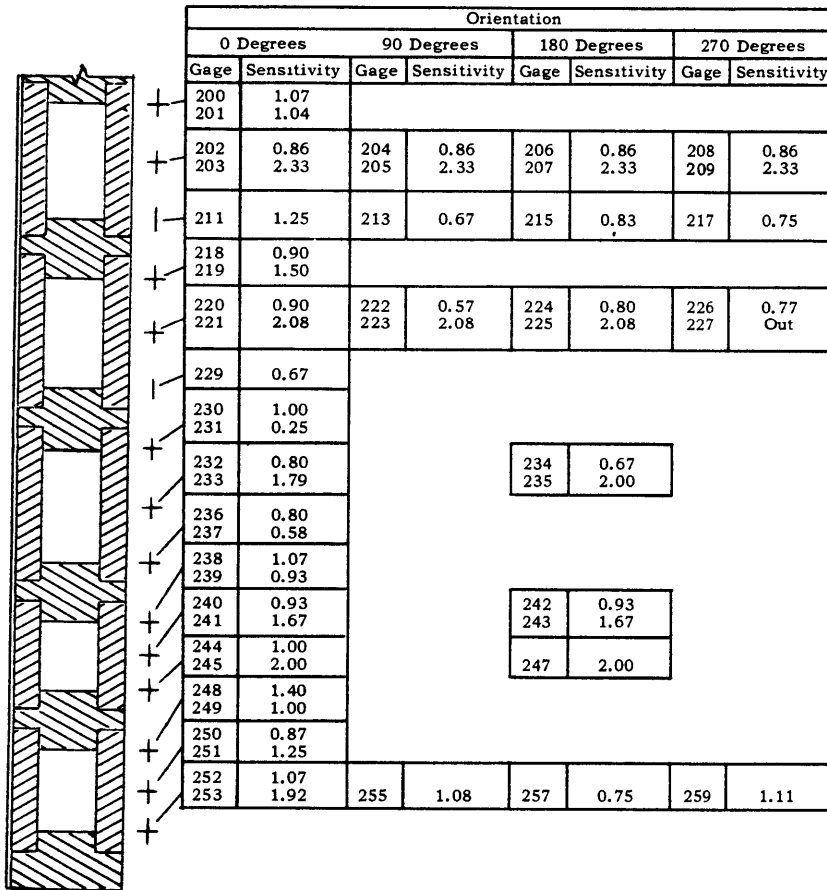


Figure 8c - Model DSRV-13

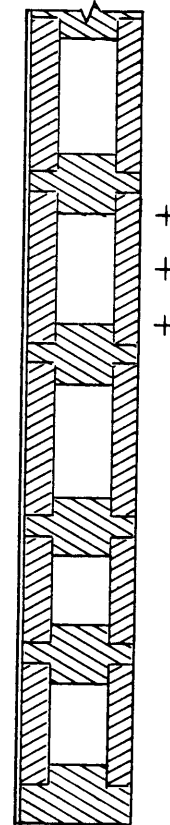


Figure 8d - Model DSRV-14



Figure 9a - Before Collapse

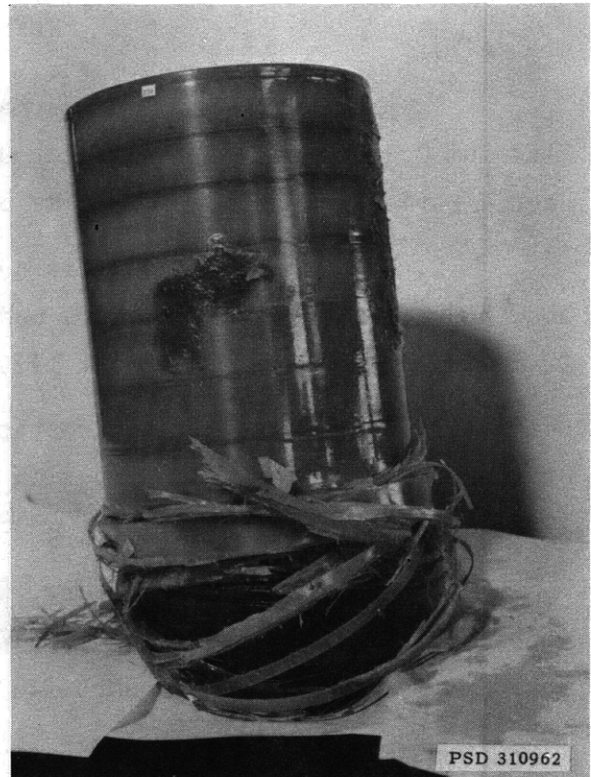


Figure 9b - After Collapse

Figure 9 - Model DSRV-11 before and after Collapse



Figure 10a - Model DSRV-12



Figure 10b - Model DSRV-13



Figure 10c - Model DSRV-14

Figure 10 - Models DSRV-12, DSRV-13, and DSRV-14 after Collapse

REFERENCES

1. Krenzke, M. A. and Kiernan, T. J., "Structural Development of a Titanium Oceanographic Vehicle for Operating Depths of 15,000 to 20,000 Feet," David Taylor Model Basin Report 1677 (Sep 1963).

2. Krenzke, M. A. and Kiernan, T. J., "Tests of Ring-Stiffened and Sandwich Composite Cylinders under External Hydrostatic Pressure," David Taylor Model Basin Report 1725 (Sep 1963).

3. Bryant, A. R., "Hydrostatic Pressure Buckling of a Ring-Stiffened Tube," Naval Construction Research Establishment Report NCRE/R 306 (1954).

4. Hom, K. and Blumenberg, W. F., "Hydrostatic Tests of Structural Models for Preliminary Design of a Web-Stiffened Sandwich Pressure Hull," David Taylor Model Basin Report 1763 (Sep 1963).

5. Krenzke, M. A., "Hydrostatic Tests of Conical Reducers between Cylinders with and without Stiffeners at the Cone-Cylinder Junctions," David Taylor Model Basin Report 1187 (Feb 1959).

6. Krenzke, M. A. and Short, R. D., "Graphical Method for Determining Maximum Stresses in Ring-Stiffened Cylinders under External Hydrostatic Pressure," David Taylor Model Basin Report 1348 (Oct 1959).

7. Myers, N. C. and Lee, G. D., "Investigation of Structural Problems with Filament Wound Deep Submersibles," H. I. Thompson Fiber Glass Company First Quarterly Report for Bureau of Ships (Apr 1963).

8. Nott, J. A., "Axisymmetric Stresses in Orthotropic, Web-Stiffened Sandwich Cylinders Loaded with Uniform External Pressure," David Taylor Model Basin Report 1859 (in preparation).

INITIAL DISTRIBUTION

Copies		Copies	
25	CHBUSHIPS	3	DIR, Plastics Tech Eval Center, Picatinny Arsenal, Dover
	9 Polymer, Fiber & Pack Sec (Code 634C)		
	1 Lab Mgt (Code 320)	1	CDR, USNOTS (Code 5557), China Lake
	3 Tech Lib (Code 210L)		
	1 Struc Mech, Hull Mat & Fab (Code 341A)	1	US Naval Ordnance Test Sta (P-8082) Pasadena, California
	1 Matls. Fuels & Cold Weather (Code 342A)		
	1 Prelim Des Br (Code 420)	20	DDC
	1 Prelim Des Sec (Code 421)		
	1 Ship Protec (Code 423)	1	CO & DIR, USNEES
	1 Hull Des Br (Code 440)	1	CO & DIR, USNUSL
	1 Sci & Res Sec (Code 442)	1	CO & DIR, USNEL
	1 Struc Sec (Code 443)	1	CO, USNROTC & NAVADMIN U, MIT
	2 Sub Br (Code 525)	1	CO, USNUOS
	1 Hull Arrgt, Fittings & Preserv (Code 633)		
	1 Pres Ves Sec (Code 651F)	1	DIR of Def R & E, Attn: Tech Lib
1	CHBUDOCKS, Attn: C-423	1	
4	CHONR	2	NAVSHIPYD PTSMH
	1 Res Coordinator (Code 104)	1	O in C, PGSCOL, Webb Inst
	1 Matl Sci Div (Code 419)	1	Dir, APL, Univ of Wash, Seattle
	1 Struc Mech Br (Code 439)		
	1 Undersea Prog (Code 466)	1	NAS, Attn: Comm on Undersea Warfare
4	CNO	1	CO & DIR, USMDL
	1 Tech Anal & Adv Gr (Op 07T)	2	Commanding General Aeronautical Systems Div (ASRCNC-1) Wright Patterson Air Force Base, Ohio
	1 Plans, Prog & Reg Br (Op 311)		
	1 Sub Program Br (Op 713)		
	1 Tech Support Br (Op 725)		
2	CO, U.S. Naval Applied Sci Lab (Code 9350)	1	WHOI
6	CHBUWEPS	1	1 Mr. J. Mavor
	1 (Code RRMA)	1	Dr. R. DeHart, SWRI
	1 (Code RMMP-23)	1	Mr. J. L. Mershon, AEC
	4 Special Projects Office		
2	CDR, USNOL	1	Aerojet-General Corp, (Mr. S. Stokes) Azusa, California
	1 W Dept		
	1 WM Div		
3	DIR, USNRL	1	NARMCO Research & Dev Div of Telecomputing Corp., San Diego, Calif (Mr. B. Duft)
	1 (Code 2027)		
	1 (Code 6120)		
	1 (Code 6210)		

Copies

1 IIT Research Institute
(Dr. J. W. Dally)
Illinois Inst of Tech
Chicago, Ill

1 Gen Motors Corp. (Dr. R. B.
Costello) Def Systems Div,
Santa Barbara Lab
Santa Barbara, Calif.

1 Battelle Memorial Inst
(Dr. R. Leininger)
Columbus, Ohio

1 H. I. Thompson Fiberglass
(Mr. N. Meyers)
Gardena, Calif.

1 Owens-Corning Fiberglass Corp.
(Mr. R. J. Weaver)
Washington, D. C.

1 U.S. Rubber Research Center
(Mr. E. Francois, Jr.)
Wayne, N. J.

1 Shell Chemical Co. (Mr. R. E.
Bayes), Plastics & Resin
Div, New York, N. Y.

1 North American Aviation Inc.
(Mr. R. Gorcey)
Rocketdyne Div
Canoga Park, Calif.

1 Hercules Powder Co
(Mr. J. A. Scherer)
Wilmington, Del.

1 Brunswick Corp. (Mr. W. McKay)
Marion, Va.

1 Douglas Aircraft Corp.
(Mr. J. H. Cunningham)
Missile & Space Systems Div.
Santa Monica, Calif.

1 Goodyear Aircraft Corp.
1210 Massillon Rd
Akron, Ohio

1 A. O. Smith Corporation
(Mr. W. A. Deringer)
Milwaukee, Wisconsin

1 University of Ill.
(Prof H. R. Corten)
Dept of T & M
Urbana, Ill

Copies

1 AVCO Corp.
Undersea Projects
Directorate
Wilmington, Mass

1 Union Carbide Plastics Corp.
(Mr. Charles Platt)
Brunswick, N. J.

MIT LIBRARIES DUPL
3 9080 02753 0309

MAR 04 1987